PHYSICAL REVIEW B VOLUME 40, NUMBER 9 15 SEPTEMBER 1989-II

Wave-vector dependence of Raman scattering intensity in folded modes of long-period α-SiC

S. Nakashima and K. Tahara
Department of Applied Physics, Osaka University, Yamadaoka, Suita, Osaka 565, Japan

(Received 22 May 1989)

It is found that the relative Raman intensity of several folded transverse-acoustic modes in silicon carbide polytypes varies markedly with the scattering wave vector q of the phonons under off-resonance conditions. A simple expression for the q-dependent intensity of Raman scattering is derived, based on the bond-polarizability concept. Using atomic displacements obtained from a linear-chain model, the variation of the intensity with q is calculated. The results agree well with the experimental results for $6H$, $8H$, $15R$, and $21R$ polytypes. This agreement indicates that the bond polarizability approximation is valid for α-SiC.

I. INTRODUCTION

In the first ordered Raman scattering process in crystals, only phonons which satisfy the wave-vector–conservation rule are observed. Since the wave vector of the phonons relevant to the scattering (scattering wave vector) is small compared with the size of the Brillouin zone, it is usually neglected. However, this is not always valid, and the finite-wave-vector (q) effect is observed in (i) polariton scattering,[1] (ii) resonant Raman scattering,[2] (iii) scattering from plasmon–LO-phonon coupled modes due to the charge-density mechanism,[3] and (iv) scattering from folded modes in long-period superlattices.[4]

Recently, it has been found that for silicon carbide (SiC) polytypes the intensity of the weak partner in doublets, which are the folded phonon modes of the transverse-acoustic (TA) branch, depends markedly on the magnitude of q, even under off-resonance conditions.[5] This dependence should be related to the drastic variation of atomic displacement patterns as q changes. In the present work the model of Raman scattering intensity for $q=0$ phonons is extended to finite q phonons. The variation of the relative intensity of partners in the doublets with changes in q has been measured in the $15R$, $6H$, $8H$, and $21R$ polytypes of SiC. The relative intensity and frequency splitting of the doublets have been calculated and compared with experimental results. In this calculation a linear-chain model is used with refined force-constant parameters obtained from the preceding paper (hereafter referred to as I). Good agreement was obtained between the calculated and experimental results. This agreement indicates that the model of the Raman scattering intensity for phonons with finite wave vectors, based on the bond-polarizability approximation, is valid for SiC crystals.

II. RAMAN SCATTERING INTENSITY

Raman scattering is treated as radiation from oscillating dipoles induced by the incident light, of which the electric field is given by

$$E_i = E_l \exp[i(k_i x - \omega_i t)] \,, \tag{1}$$

where k_i and ω_i are the wave vector and frequency, respectively.

First, a one-dimensional model is considered with the assumption that the electronic polarizability is a function of only the bond separation. The dipole moment arising from the jth bond in the nth unit cell is written as

$$p(n|j) = \alpha(n|j) E_l \exp\{ i[k_i x(n|j) - \omega_i t] \} \,. \tag{2}$$

The bond polarizability $\alpha(n|s)$ is expanded in a power series of the bond-length variation $\Delta r(n|j)$ as

$$\begin{aligned} \alpha(n|j) &= \alpha^0(n|j) + \frac{\partial \alpha}{\partial r(n|s)_0} \Delta r(n|j) + \dots \\ &= \alpha^0(j) + \alpha_s^1 [u(n|j) - u(n|j+1)] + \dots \,, \end{aligned} \tag{3}$$

where $u(n|j)$ and $u(n|j+1)$ are the displacements of the end atoms of the bond. The first derivative of the polarizability α^1 is evaluated at the equilibrium separation between the end atoms. The second term of Eq. (3), which is related to the Raman scattering process, provides a dipole,

$$\Delta p(n|j) = \alpha_s^1 [u(n|j) - u(n|j+1)] E_i \,. \tag{4}$$

When setting

$$u(n|j) = u(j) \exp\{ i[\omega(q)t - qx_n] \} \tag{5a}$$

and

$$x(n|j) = x_n + x_j \,, \tag{5b}$$

where $\omega(q)$ is the frequency of the phonon, $u(j) \equiv u(x_j)$ and x_n is the position of the nth unit cell. Evoking the conservation rules of energy and momentum,

$$\omega_s = \omega_i - \omega(q) \quad \text{and} \quad k_s = k_i - q \,. \tag{6}$$

Using Eqs. (5) and (6), Eq. (4) can be rewritten as

$$\Delta p(n|j) = \alpha_s^1 E_l [u(j) - u(j+1)] e^{iqx_j} e^{i[k_s x(n|j) - \omega_s t]} \,. \tag{7}$$

Raman scattering intensity is related to the amplitude of the polarization wave having (ω_s, k_s), which is given by

$$p(q)=\frac{1}{N}\sum_{n,j}\Delta p(n|j)e^{-i[k_s x(n|j)-\omega_s t]}$$
$$=\sum_j \alpha_j^1[u(j)-u(j+1)]e^{iqx_j}E_l \ , \qquad (8)$$

where N is the number of unit cells in the crystal. For the phonon mode $(\omega(q),q)$, the Raman scattering intensity is obtained by

$$W=\frac{n(\omega)+1}{\omega}A|\Delta p(q)|^2 \ , \qquad (9)$$

where A is a proportional constant and $n(\omega)$ is the Bose factor. Equation (8) can be easily extended to three-dimensional crystals. The amplitude of light scattered in the k_s direction by a phonon propagating in the direction q is given by

$$p(q)=[e_s\cdot\Delta\mathbf{p}(q)]E_l=(e_s\cdot\alpha_s^1\cdot e_i)E_l \ , \qquad (10)$$

and

$$\alpha_{\rho\sigma}^1(q)=\sum_j\left\{\frac{\partial[\alpha_j]_{\rho\sigma}}{\partial x_j}\Delta x_j+\frac{\partial[\alpha_j]_{\rho\sigma}}{\partial y_j}\Delta y_j+\frac{\partial[\alpha_j]_{\rho\sigma}}{\partial z_j}\Delta z_j\right\}e^{iqr_j} \ , \qquad (11)$$

where e_i (e_s) is the polarization of the incident (scattered) light and $\Delta x_j=u_x(j)-u_x(j+1)$ is the x component of the relative displacement for the end atoms of the jth bond. The bond Raman polarizability $\partial[\alpha_j]/\partial x_j$ is given by Eq. (17) of Ref. 6. Equations (8) and (9) are equivalent to the expression obtained for the folded modes in superlattices by Jusserand *et al.*[7] The SiC polytypes are formed from double layers of Si-C. These are stacked together in such a way that each silicon atom is surrounded by four carbon atoms that form a tetrahedron and vice versa. The configuration of the second neighbors consists of two types: a hexagonal h like that of atom B in the sequence ABA and a cubic configuration k similar to that of atom B in the sequence ABC.

The configurations of the bonds in SiC are classified into three groups with respects to the phonons propagating along the c direction.[6] The configurations of these bonding portions are (i) αB, βC, and γA, (ii) αC, βA, and γB, and (iii) $A\alpha$, $B\beta$, and $C\gamma$. Here, the positions of the carbon atoms are represented by Greek letters, while those of the silicon atoms are shown by Latin letters. The Raman tensors for groups (i) and (ii) are obtained through the summation of contributions from the three bonds. The scattering configuration employed in this work examines α_{xx}, α_{yy}, and α_{xy}, for the phonons whose displacements lie within the planes perpendicular to the c direction. For the folded TA mode the tensor components of the bond Raman polarizability, α_{xx}, α_{yy}, and α_{xy}, have the same magnitude and differ only in their sign for groups (i) and (ii). In this case, Eq. (11) is reduced to

$$\alpha_{\rho\sigma}^1(q)=c\sum_{j=\text{even}}\pm[u(j)-u(j+1)]\exp(iqz_j) \ , \qquad (12)$$

where c is the xy component of the Raman tensor for the E-type mode.

From Eq. (12) it follows that the relative Raman intensity of the folded modes that belong to the same branch does not depend on the Raman polarizability, but only on the atomic displacements. This conclusion is valid only when the difference of the Raman polarizability tensors between hexagonal and cubic configurations can be neglected.

A linear-chain model is used in the calculations of the displacements of the atomic planes. The determination of the force-constant parameters for the transverse phonons in SiC is described in I. The displacements of the atomic planes are obtained by solving the following equations of motion:

$$M_j\omega^2 u(n|j)=\sum_{r,s}D_{j,j+s}^r u(n+r|j+s) \ , \qquad (13)$$

where $D_{j,j+s}^r$ is related to the interplanar force between the jth and $(j+s)$th planes $K_{j,j+s}$, and M_j is the mass of the jth atomic plane. For nH and $3nR$ polytypes, $2n$ equations of motion are obtained. Solutions of the exponential form are sought, such as

$$u(n|j)=u(j)\exp(-iqx_n), \quad u(j)=A_j\exp[i\phi(j,q)] \ , \qquad (14)$$

$$A_j=|A_j|\exp[i\alpha(q)] \ , \qquad (15)$$

and

$$\phi(j,q)=-qx_j+\phi_j(q) \ , \qquad (16)$$

where $x_j=jc$ for carbon atoms and $x_j=(j+\frac{3}{4})c$ for silicon atoms. The condition that Eq. (13) has nontrivial solutions results in the dispersion relation

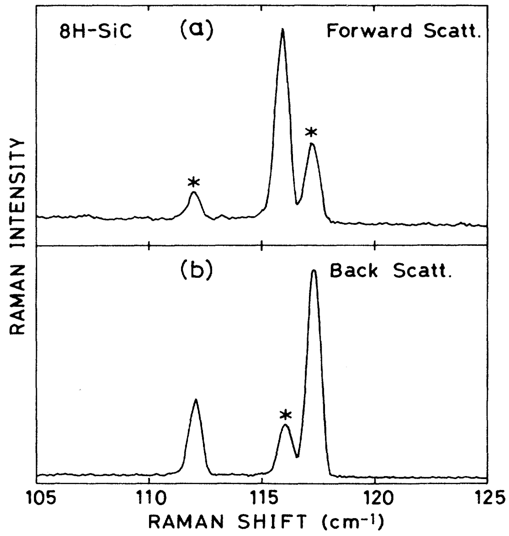

FIG. 1. Raman spectra of the $q(\frac{1}{4})$ mode in the TA branch of the $8H$ polytype observed with (a) forward scattering and (b) backscattering geometries. The bands marked with an asterisk are signals due to the incident laser reflected from the back surface of the sample.

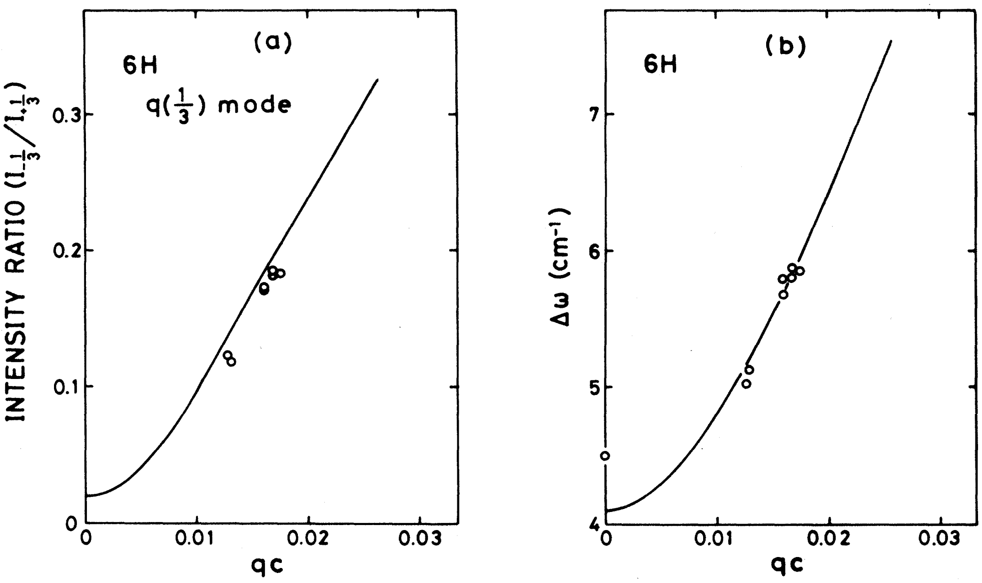

FIG. 2. (a) Intensity ratio of the lower to upper component, and (b) splitting of these components obtained for the $q(\frac{1}{3})$ mode in the TA branch of the 6*H* polytype.

$$|\delta_{ij}M_j\omega^2 - D_{ij}(q)| = 0 \ . \qquad (17)$$

The term $D_{ij}(q)$ is given in Eq. (7) of I.

III. EXPERIMENTAL RESULTS

Long-period SiC polytypes exhibit a number of Raman bands arising from the folded modes of the TA and TO branches. The folded TA modes which correspond to the phonons inside the Brillouin zone usually from doublets.[6,8] Raman scattering is measured for the most intense doublet of several SiC polytypes (6*H*, 8*H*, 15*R*, and 21*R*) with forward-scattering and backscattering configurations. The spectral slitwidth of the spectrometer is set approximately to 0.6 cm^{-1}. Thin crystal platelets having the (0001) face grown by the Acheson method are used. The direction of both the incident and scattered light is parallel to the *c* axis.

Figure 1 shows the results for the 8*H* polytype. The

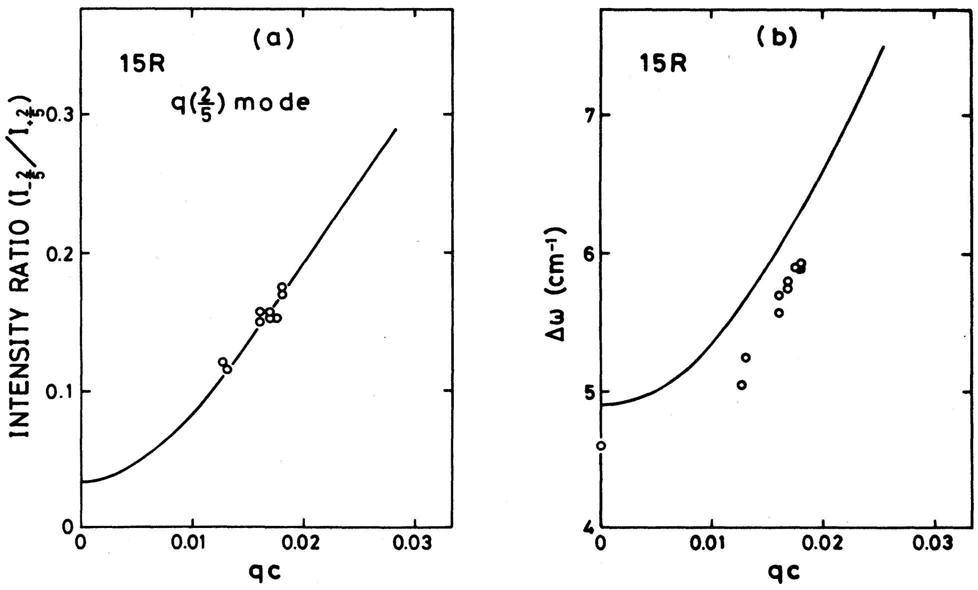

FIG. 3. (a) Intensity ratio of the lower to upper component, and (b) splitting of these components obtained for the $q(\frac{2}{5})$ mode in the TA branch of the 15*R* polytype.

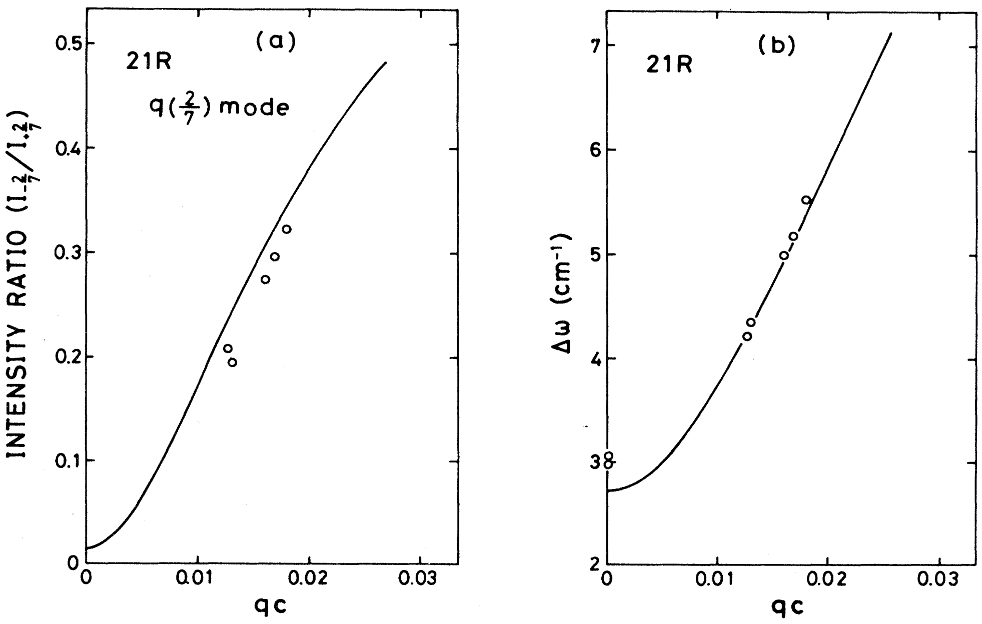

FIG. 4. (a) Intensity ratio of the lower to upper component, and (b) splitting of these components obtained for the $q(\frac{2}{7})$ mode in the TA branch of the 21*R* polytype.

peak values of the two partners are quite different. The high-frequency partner measured with a backscattering configuration has a small hump on the low-frequency side. This is a forward-scattering component due to the reflected light inside the sample. Conversely, the hump in the forward-scattering spectrum is the backscattering component. The frequencies of these peaks differ for the two configurations, implying that dispersion exists in these phonon modes.

It should be noted that the relative intensity of the low-frequency partner is very weak for the forward-scattering configuration. The intensity reduction with this configuration is not due to the formation of a polariton mode, since this doublet belongs to the E_2 representation at the Γ point and is infrared inactive.

The most intense doublets of the folded TA modes are the $q(\frac{1}{3})$ modes for 6*H*, the $q(\frac{2}{5})$ modes for 15*R*, and the $q(\frac{2}{7})$ modes for 21*R*. The phonon mode at a certain $q(\frac{2}{7})$ point in the basic Brillouin zone (BZ of the 3*C*) is hereafter denoted the $q(x)$ mode, where $x = q/q_B$ is the reduced wave vector.

Attempts at measuring the q dependence of the relative intensity and frequency splitting were made for these doublets by varying the wavelength of the argon and krypton lasers. The results obtained for 6*H*, 15*R*, and 21*R* polytypes are shown in Figs. 2, 3, and 4, respectively. The scattering wave vector q is calculated using the equation $q = 4n\pi/\lambda_i$, where λ_i is the wavelength of the incident light and n is the refractive index of SiC, set at $n = 2.69$. The intensity ratio of the low-frequency partner to the high-frequency partner increases with increasing q for these doublets. The frequency splitting of the doublets also increases as q increases. The intensity ratio and frequency splitting are calculated using Eqs. (9), (12), and (17). For these calculations use is made of the force-constant parameters (K_i and ΔK_i) listed in Table I of I. The calculated results are also shown in Fig. 2–4, represented by solid lines. Fair agreement can be seen between the calculated and experimental results for the 6*H* and 21*R* polytypes. However, a slight discrepancy is found in the frequency splitting of the 15*R* polytype.

IV. DISCUSSIONS

The marked dependence of the Raman intensity on q in a small region of q is observed for the doublets of folded TA modes consisting of partners with quite different intensities. However, no appreciable dependence is observed for folded TO modes in the polytypes studied.

To understand the variation of the Raman intensity with q, examination of the atomic displacements are made for various q's which are given by Eqs. (14) and (15). The values of $|A_j|$ and $\phi_j(q)$ calculated for the upper and lower partners of the $q(\frac{1}{3})$ doublet of the 6*H* polytype are shown in Figs. 5 and 6, respectively. The amplitude $|A_j(q)|$ and phase $\phi_j(q)$ vary remarkably with q even in a small region of q. This striking feature is also found in the $q(\frac{2}{5})$ doublet of the 15*R* polytype, the $q(\frac{2}{7})$ doublet of 21*R*, and the $q(\frac{1}{4})$ doublet of 8*H* (figures are not shown). The phase and amplitude of other folded TA modes vary slightly with q in the region of $q < 0.1$. The calculated results show that for the $q(\frac{2}{3})$ modes of the 6*H* polytype, whose intensities are almost zero, the phase $\phi_j(q)$ varies with q. However, the absolute intensities are still very small for a finite q. The doublets which show the remarkable intensity variation with q correspond to the strongest folded TA modes of the 6*H*, 8*H*, 15*R*, and 21*R* polytypes. However, this remarkable intensity variation is not limited to the strongest doublets of a polytype. The results of computations for the 27*R* polytype suggest that the intensities of doublets at 95 and 97 cm^{-1} also vary appreciably with q, although their intensities are weak.

Figures 5(a) and 5(b) show that the variation of $|A_j|$ with x_j decreases as q increases.

As seen in Fig. 6, the values of $\phi_j(q)$ versus x_j approach a straight line as q increases, which can be expressed $\phi_j(q)=(3c)^{-1}\pi x_j$, where c is the unit-cell length along the [111] direction of the 3*C* polytype. At $qc=0.05$, the wave forms of the upper and lower branches are close to that of the traveling wave at $x=0.33$ in 3*C*-SiC, for which there is no hexagonal configuration, and the difference of the force constants between the hexagonal and cubic configurations (ΔK_i) is taken to be zero. The notable variation in the phase and amplitude of certain doublets is responsible for the variation in their relative intensity in a small-q region. It is interesting to note that the sum of the intensities of two partners in a doublet is almost constant for any q. Calculated results show that the increase in the intensity of one partner causes a decrease in that of the other partner.

Noticeable q dependence in the phase is also found for the folded TO modes, e.g., the $q(\frac{4}{5})$ modes of the 15*R* polytype. The calculated intensity ratio of the higher- to lower-frequency component was 3.8×10^{-4} at $q=0$ and 1.1×10^{-3} at $qc=0.017$. However, the intensity varia-

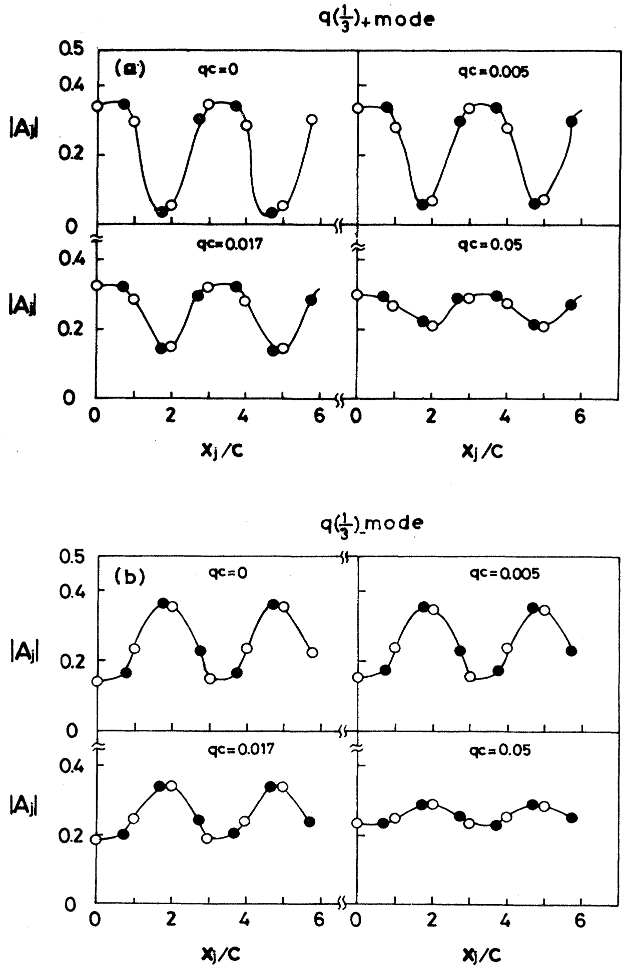

FIG. 5. The displacement amplitudes $|A_j|$ of silicon and carbon planes of the 6*H* polytype for (a) the $q(\frac{1}{3})_+$ mode at 145 cm^{-1} and (b) the $q(\frac{1}{3})_-$ mode at 141 cm^{-1}. The solid lines were drawn to guide the eye. Silicon and carbon planes are shown by open and solid circles, respectively.

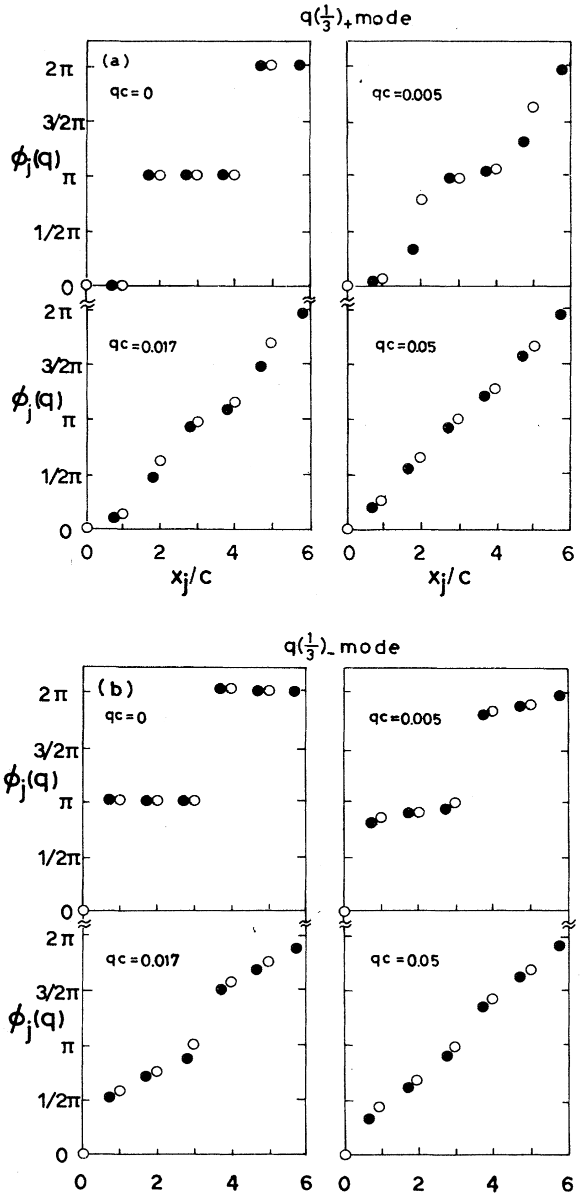

FIG. 6. The phases $\phi_j(q)$ of silicon and carbon planes for the 6*H* polytype are shown for several q's for (a) the $q(\frac{1}{3})_+$ mode at 145 cm^{-1} and (b) the $q(\frac{1}{3})_-$ mode at 141 cm^{-1}.

tion was hardly observed, since the intensity of the weak partner is too small and the folded TO modes are too broad for the doublet to be resolved.

So far, the relative Raman-intensity profile of folded modes has been used to determine the polytype structure. The results of the present work indicate that it is necessary to take into account the q dependence of the intensity in the structural determination, especially for longer-period polytypes.

The strong q dependence of the Raman scattering intensity should not be restricted to polytype crystals. It is also expected to be present in crystals having a long period or complicated unit-cell structure.

V. CONCLUSIONS

It has been found that the Raman scattering intensity in SiC polytypes varies strikingly with the momentum transfer q for certain folded TA modes. The calculated Raman scattering intensities as a function of q were found to be in agreement with the experimental results. Since the q dependence is sensitive to the choice of eigenvectors, the intensity analysis can be used to test the validity of the model of lattice dynamics used. The agreement between the experimental and calculated results demonstrates that the bond-polarizability concept for the explanation of the Raman intensity is valid for SiC.

---

[1] E. Burstein and F. De Martini, *Polaritons* (Pergamon, New York, 1974).

[2] R. H. Martin, in *Light Scattering in Solids,* edited by M. Balkanski (Flammarion, Paris, 1971), p. 25.

[3] H. Yugami, S. Nakashima, K. Sakai, H. Kojima, M. Hangyo, and A. Mitsuishi, J. Phys. Soc. Jpn. **56**, 1881 (1987).

[4] See M. V. Klein, IEEE J. Quantum Electron. **QE-22**, 1760 (1986).

[5] S. Nakashima and K. Tahara, in *Proceedings of the 11th International Conference on Raman Spectroscopy, London, 1988,* edited by R. J. H. Clark and D. A. Long (Wiley, New York, 1988), p. 333.

[6] S. Nakashima, H. Katahama, Y. Nakakura, and A. Mitsuishi, Phys. Rev. B **33**, 5721 (1986).

[7] B. Jusserand, D. Paquet, F. Mollot, F. Alexandre, and G. Le Roux, Phys. Rev. B **35**, 2808 (1987).

[8] C. H. Hodges, Phys. Rev. **187**, 994 (1969).